

# RSC Advances



This is an *Accepted Manuscript*, which has been through the Royal Society of Chemistry peer review process and has been accepted for publication.

*Accepted Manuscripts* are published online shortly after acceptance, before technical editing, formatting and proof reading. Using this free service, authors can make their results available to the community, in citable form, before we publish the edited article. This *Accepted Manuscript* will be replaced by the edited, formatted and paginated article as soon as this is available.

You can find more information about *Accepted Manuscripts* in the [Information for Authors](#).

Please note that technical editing may introduce minor changes to the text and/or graphics, which may alter content. The journal's standard [Terms & Conditions](#) and the [Ethical guidelines](#) still apply. In no event shall the Royal Society of Chemistry be held responsible for any errors or omissions in this *Accepted Manuscript* or any consequences arising from the use of any information it contains.

## COMMUNICATION

## Interaction effect between Cr(OH)<sub>3</sub> passive layer formation and inhibitor adsorption on 3Cr steel surface

Cite this: DOI: 10.1039/x0xx00000x

Received xxx

Accepted xxx

DOI: 10.1039/x0xx00000x

www.rsc.org/

Jinyang Zhu,<sup>a</sup> Lining Xu,<sup>b</sup> Minxu Lu,<sup>a</sup> Lei Zhang,<sup>a</sup> and Wei Chang<sup>b</sup>

**Passive layer formation and inhibitor adsorption on the 3Cr steel surface in the absence of an interface inhibitor, i.e. benzamide, has been investigated. Above a threshold of roughly 600 mM, benzamide rapidly adsorbed on the substrate surface and significantly inhibited the formation of passive layer.**

In the modern oil production systems, CO<sub>2</sub>-enhanced oil recovery (EOR) has attracted more attentions owing to its positive contributions to geological storage of Carbon.<sup>1</sup> However, it is a serious and challenging problem in the oil production, gathering and transportation processes when CO<sub>2</sub> meets water.<sup>2,3</sup> Recently, corrosion inhibitor has become an effective way to control the CO<sub>2</sub> corrosion.<sup>4-6</sup> Interface inhibitors, which control corrosion by forming a protective barrier at the metal/environment interface, are an important group of inhibitors. Amide inhibitors belong to interface inhibitors.<sup>7</sup> Amino as polar group can provide lone pair electrons, forming the coordination bond with the empty d orbital in iron atoms.<sup>8</sup> Therefore, a complete layer of inhibitor firmly adsorbs on the steel surface, thus inhibiting the corrosion of the substrate.

3Cr steel is a new type of low alloy steel developed for using in CO<sub>2</sub> environments, which is obtained by adding 3 % chromium to traditional carbon steel. In recent years, researchers have investigated the ability of this steel to control CO<sub>2</sub> corrosion.<sup>9-11</sup> One previous study reported that 3Cr steel can improve CO<sub>2</sub> corrosion resistance by a factor of 3–10 and maintain a cost less than 1.5 times higher than that of conventional grades of carbon steel.<sup>12</sup> Although 3Cr steel has such excellent corrosion resistance, it is not stainless steel. Corrosion inhibitor is needed in the corrosion of 3Cr steel pipe in some critical conditions. As mentioned, interface inhibitors can adsorb on the steel surface. Meanwhile, a Cr-rich passive layer will

form on the 3Cr steel surface as a result of 3% Cr addition.<sup>13</sup> Then, whether the presence of interface inhibitors will affect the formation of this passive layer or not? Presently, little related research has been reported.

Therefore, the aim of this work is to investigate the impact of interface inhibitors on the passive layer formation. In this study, the anodic polarization curves of 3Cr steels in CO<sub>2</sub>-saturated solutions with various benzamide concentrations were measured. Material tested was 3Cr low alloy steel with a chemical composition (wt %): 0.07 C, 0.2 Si, 0.55 Mn, 2.96 Cr, 0.15 Mo, 0.03 Nb, 0.03 V and Fe balance. The working electrode is made from 3Cr steel in the form of cylindrical rods with an apparent surface area of 1 cm<sup>2</sup>. The composition of the test solution is listed as follows (mM): 432.8 NaCl, 24.8 CaCl<sub>2</sub>, 8.6 KCl, 9.5 MgCl•6H<sub>2</sub>O and 1.4 NaSO<sub>4</sub>. The inhibitor used in this work was a simple amide inhibitor, i.e. benzamide, belonging to interface inhibitors. The chemical structure of this inhibitor is given below:

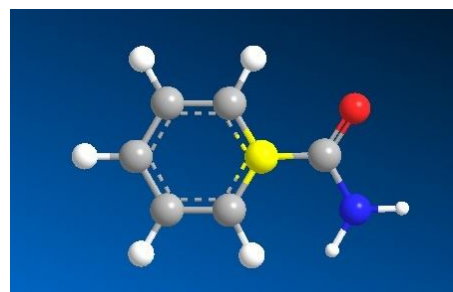
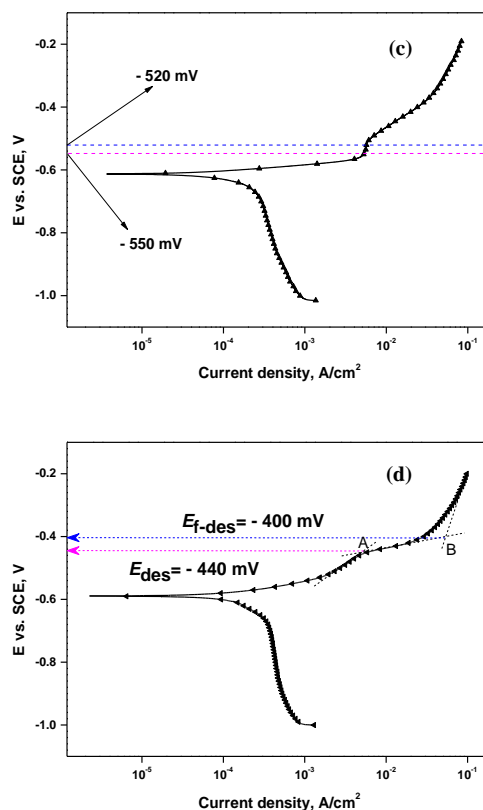
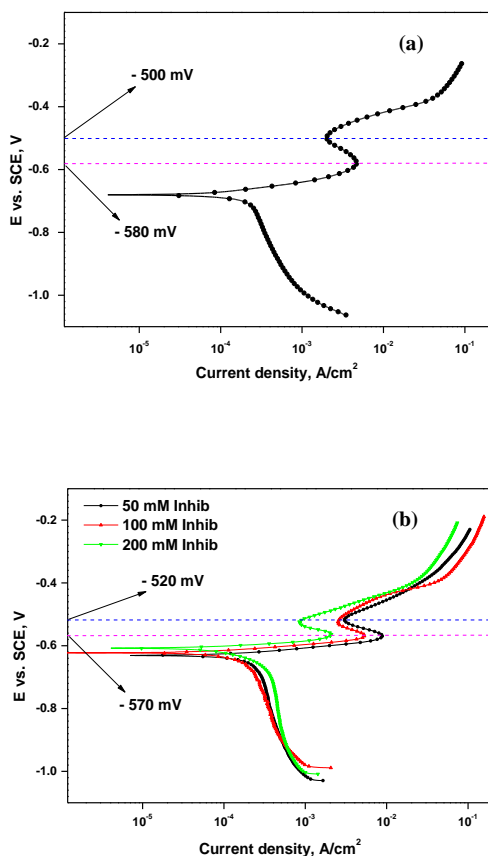


Fig. 1. Molecular structure of benzamide.

Polarization curves for 3Cr steel RDE (1000 rpm) in CO<sub>2</sub>-saturated solutions with various inhibitor concentrations are shown in Fig. 2. Fig. 2a shows that the anode polarization curve for 3Cr steel in the solution devoid of inhibitor exhibited a decrease in current between -580 mV and -500 mV. This phenomenon was identified as semi-passivation or prepassivation, which was probably related to the formation of a Cr-rich passive layer on 3Cr steel.<sup>13</sup> The experimental verification of this Cr-rich layer will be given in the following page.

When the inhibitor was added into the solutions (50 mM, 100 mM, and 200 mM), the anode polarization curves for 3Cr steel were similar with that in Fig. 2a, in which the decreases in current between -570 mV and -520 mV were observed (Fig. 2b). However, if the inhibitor concentration reached 600 mM, the decrease of current in the anodic domain disappeared. Instead, a potential plateau characterized by a rapid current rise was observed (Fig. 2d). Cao<sup>14,15</sup> believed that this potential plateau was probably caused by the inhibitor desorption from iron surface as it was anodically polarized. In Fig. 2d, the potential at point A was the desorption potential,  $E_{des}$ , corresponding to the potential at which the desorption rate was equal to the adsorption rate for the inhibitor. The potential at point B was  $E_{f-des}$ , at which the inhibitor desorption was basically finished. Fig. 2c shows the polarization curve for 3Cr steel in the solution containing 400 mM inhibitor. There is no current decrease and no potential plateau in its anodic domain. A small step was observed, which was probably caused by the combined effect of passive layer formation and inhibitor adsorption.

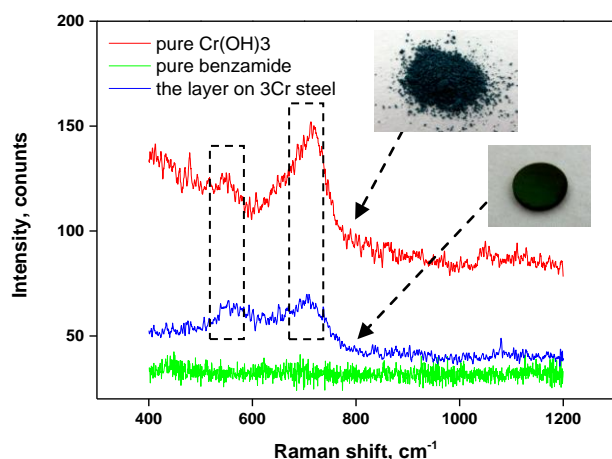


**Fig. 2.** Potentiodynamic polarization curves for 3Cr steel RDE (1000 rpm) in CO<sub>2</sub>-saturated solutions with various inhibitor concentrations at a scan rate of 0.2 mV/s at 80 °C. (a) Blank; (b) 50-200 mM Inhib; (c) 400 mM Inhib; (d) 600 mM Inhib.

To investigate what substance had formed on the 3Cr steel surface and caused the decrease in current in anodic polarization curves when the inhibitor concentration was below 200 mM, Raman spectroscopy and X-ray photoelectron spectroscopy (XPS) measurements were conducted. In Fig. 2b, one potential was chosen, -550 mV, which was between -570 mV and -520 mV. The 3Cr steel sample for XPS and Raman tests was polarized from the open circuit potential (OCP) to -550 mV in the solution containing 50 mM inhibitor, and then quickly extracted from the solution.

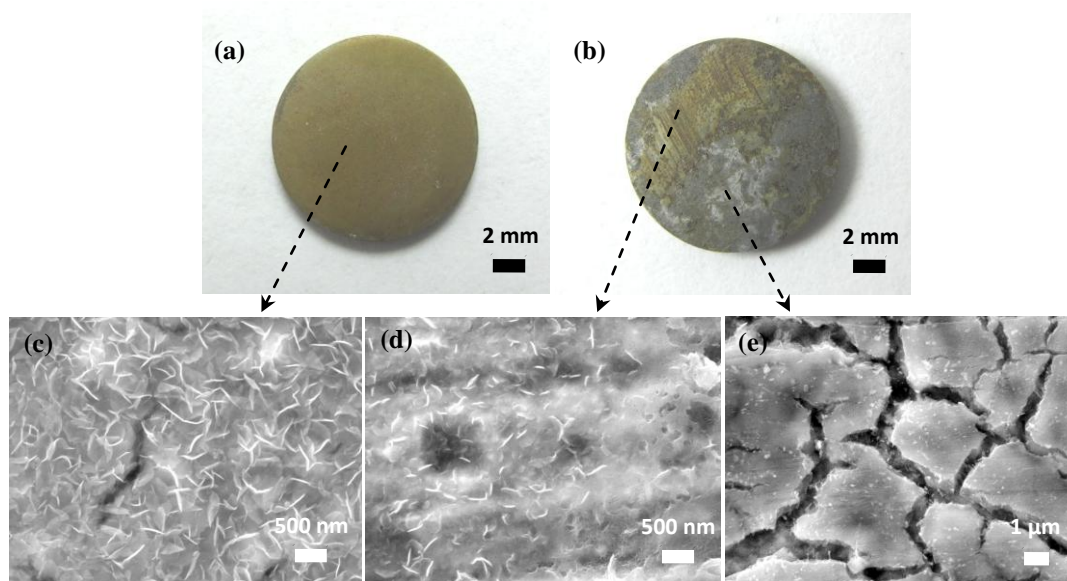
Fig. 3 depicts the Raman spectra of pure Cr(OH)<sub>3</sub> powders, pure benzamide, and the layer on the 3Cr steel sample that was polarized to -550 mV at 50 mM inhibitor concentration. The pure Cr(OH)<sub>3</sub> powders were prepared from ammonia and Cr(NO<sub>3</sub>)<sub>3</sub>. As shown in Fig. 3, regarding the layer on the 3Cr steel surface, two sets of peaks located at 578 cm<sup>-1</sup> and 701 cm<sup>-1</sup> were observed and were consistent with the peaks (555 cm<sup>-1</sup>, 713 cm<sup>-1</sup>) in the Cr(OH)<sub>3</sub> powders. Moreover, no peak was observed on the spectra of the pure benzamide, indicating that the inhibitor did not influence the Raman spectra of the steel surface. On the other hand, XPS was used to further confirm the composition of this passive layer. As shown in Fig. 4, the Cr 2p high resolution spectra of this passive layer reveals an Cr 2p<sub>1/2</sub> peak at a binding energy of 577.4 eV and an Cr 2p<sub>3/2</sub> peak at 587.1 eV, both corresponding to Cr(OH)<sub>3</sub>.<sup>16,17</sup> Therefore, it can be suggested that the passive layer which covered on the 3Cr steel surface mainly consisted of Cr(OH)<sub>3</sub>. As the polarization progressed, Cr(OH)<sub>3</sub> continually formed and covered on the 3Cr

steel surface, thereby causing the decrease in current observed in the anode polarization curves in Fig. 2b.



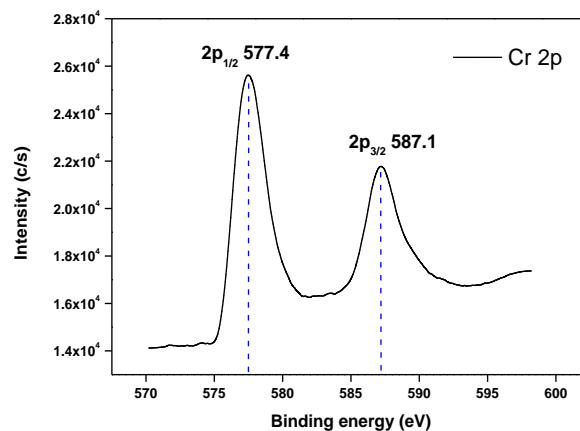
**Fig. 3.** Raman spectra of pure Cr(OH)<sub>3</sub> powders, pure benzamide, and the layer on the 3Cr steel sample that was polarized to -550 mV in CO<sub>2</sub>-saturated solution with 50 mM inhibitor.

In Fig. 2d, two potentials were chosen: one was  $E_a$  (-460 mV) which was slightly below  $E_{des}$ , the other was  $E_b$  (-420 mV) which was between  $E_{des}$  and  $E_{f-des}$ . The two 3Cr steel samples were polarized from the OCP to  $E_a$  and  $E_b$  in the solution containing 600 mM inhibitor, respectively, and then quickly extracted from the solution. Fig. 5 shows the macro and micro morphologies of these two 3Cr steel samples. As shown in Fig. 5a, the 3Cr steel surface that polarized to  $E_a$  was smooth and dark yellow. By contrast, a much rougher surface showed on the 3Cr steel sample polarized to  $E_b$  and most of the surface was dark gray (Fig. 5b).



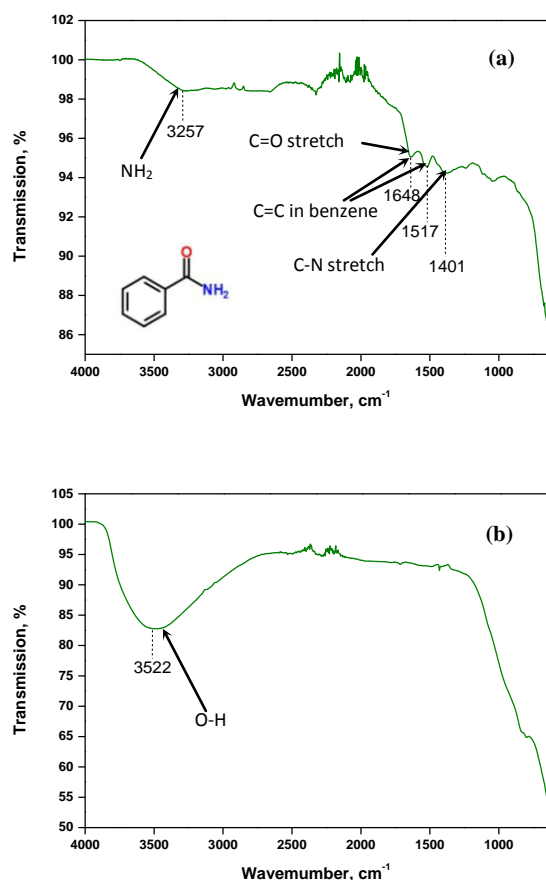
**Fig. 5.** Macro morphologies of the layer on the 3Cr steel sample that was polarized to (a) -460 mV and (b) -420 mV in CO<sub>2</sub>-saturated solution with 600 mM inhibitor; (c, d, and e) micro morphologies of the layer in different regions where the arrow is pointing.

Fig. 5c shows the field-emission scanning electron microscopy (FE-SEM) image of the dark yellow area in Fig. 4a. It was found that there were many sub-micro floccules with the sizes of about 400 nm covering on the substrate surface. This sub-micro layer was probably related to the adsorption of the inhibitor on the steel surface. Figs. 5(d and e) show the FE-SEM images of different regions in Fig. 5b. As shown in Fig. 5d, a layer with a few floccules, which was similar with that in Fig. 5c, covered on the steel surface of the yellow area in Fig. 5b. However, the coverage-ratio of these floccules in Fig. 5d was significantly below that in Fig. 5c. Moreover, in the dark gray area of Fig. 5b, no floccules were observed and a cracked corrosion film covered on the steel surface (Fig. 5e). This indicates that the inhibitor was desorbing from the steel surface when the steel was polarized to  $E_b$ .



**Fig. 4.** The Cr 2p XPS spectra obtained from the layer on the 3Cr steel sample that was polarized to -550 mV in CO<sub>2</sub>-saturated solution with 50 mM inhibitor.

As mentioned before, the potential plateau in Fig. 2d was probably caused by the inhibitor desorption.  $E_a$  was below  $E_{des}$ . Therefore, it can be speculated that the floccules on the steel surface polarized to  $E_a$  were probably the inhibitor. To determine the composition of the floccules, attenuated total reflection infrared spectroscopy (ATR-IR) measurements were realized on the steel surface in Fig. 5a. ATR-IR has become a kind of beneficial tool and means for analyzing surface properties. Fig. 6(a) shows the ATR-IR spectrum of the floccules layer in the frequency range (650–4000  $\text{cm}^{-1}$ ). The band located at 1648  $\text{cm}^{-1}$  and 1571  $\text{cm}^{-1}$  corresponds to the C=C bond in benzene ring. The band at 1648  $\text{cm}^{-1}$  also corresponds to the C=O stretching vibrations of amide. There was a band at 1401  $\text{cm}^{-1}$  which was due to the C-N stretching vibrations of amide. A broad peak in the range of 3200–3600  $\text{cm}^{-1}$  corresponds to the vibrational mode of N-H bond. Therefore, the spectra exhibits bands corresponding to the benzamide, indicating that the adsorbed floccules layer on the 3Cr steel surface in Fig. 5c mainly consists of the inhibitor. On the other hand, ATR-IR tests were also realized on the 3Cr steel sample that was polarized to -550 mV in  $\text{CO}_2$ -saturated solution with 50 mM inhibitor. As shown in Fig. 6(b), there was only one band at 3522  $\text{cm}^{-1}$  which corresponds to the O-H bond of  $\text{Cr}(\text{OH})_3$ , indicating that there was no inhibitor adsorbing on the steel surface. This was consistent with the results of Fig. 3.



**Fig. 6.** (a) ATR-IR spectra of the layer on the 3Cr steel surface in Fig. 5a; (b) ATR-IR spectra of the layer on the 3Cr steel sample that was polarized to -550 mV in  $\text{CO}_2$ -saturated solution with 50 mM inhibitor.

The results above demonstrated that the inhibitor concentration was a key variable governing the passive layer formation on the 3Cr steel surface. When the benzamide concentration was below 200 mM, inhibitor molecules were dispersed in the solution with a low density and could not fully cover the steel surface in a short time. An incubation period is needed for the inhibitor adsorption. The bare steel substrate was quickly corroded during this incubation period and the continuous selective dissolution of Fe from 3Cr-steel surface resulted in an enrichment of Cr on the steel surface. The enriched Cr reacted with the water at the interface and  $\text{Cr}(\text{OH})_3$  was generated. Therefore, a Cr-rich passive layer formed and covered on the steel surface, resulting in a current decrease in the anode polarization curves (Fig. 2b). That is, the presence of the inhibitor has no significant impact on the formation of  $\text{Cr}(\text{OH})_3$  passive layer below the inhibitor concentration of 200 mM. However, if the benzamide concentration reached sufficient high, such as 600 mM, inhibitor molecules could quickly aggregate at the steel/environment interface in a short time. A complete layer of inhibitor formed and adsorbed on the steel surface. This inhibitor layer could effectively inhibit the corrosion of the substrate, thereby preventing the passive layer formation. Therefore, a typical potential plateau corresponding to the inhibitor desorption was observed in Fig. 2d.

## Conclusions

In the absence of interface inhibitors, an interaction effect between the passive layer formation and the inhibitor adsorption was observed on the 3Cr steel surface. When the inhibitor concentration is below 200 mM, the presence of the inhibitor has no significant impact on the passive layer formation of 3Cr steel. However, above a threshold of roughly 600 mM, inhibitors can quickly adsorb on the steel surface and significantly inhibit the formation of  $\text{Cr}(\text{OH})_3$  passive layer.

## Notes and references

<sup>a</sup> Corrosion and Protection Center, Institute for Advanced Materials and Technology, University of Science and Technology Beijing, Beijing 100083, China.

<sup>b</sup> CNOOC Research Institute, Beijing 100027, China.

- 1 J. Zhang, Z.L. Wang, Z.M. Wang and X. Han, *Corros. Sci.*, 2012, 65, 397-404.
- 2 R. Singh, Enhanced oil recovery and  $\text{CO}_2$  corrosion a challenge, in: 2010 China International Pipeline Forum, Langfang, China, 2010, pp. 162-171.
- 3 S. Nestic, *Corros. Sci.*, 2007, 49, 4308-4338.
- 4 W. Durnie, R. de Marco, B. Kinsella, A. Jefferson and B. Pejic, *J. Electrochem. Soc.*, 2005, 152, B1-B11.
- 5 X. Jiang, Y.G. Zheng and W. Ke, *Corros.*, 2005, 61, 326-334.
- 6 V. Pandarinathan, K. Lepkova, S.I. Bailey and R. Gubner, *Corros. Sci.*, 2013, 72, 108-117.
- 7 H.Y. Du, M.X. Lu, Y.S. Wu and W.M. Wu, *Acta Metallurgica Sinica*, 2006, 42, 533-536.
- 8 T.S. Zhang, H. Zhang and H. Gao, *Corrosion Inhibitors*, second ed., Kluwer Academic Publishers, Beijing, 2008.
- 9 A. Pfennig and A. Kranzmann, *Corros. Sci.*, 2012, 65, 441-452.
- 10 M. Ko, B. Ingham, N. Laycock and D.E. Williams, *Corros. Sci.*, 2014, 80, 237-246.
- 11 Q.L. Wu, Z.H. Zhang, X.M. Dong and J.Q. Yang, *Corros. Sci.*, 2013, 75, 400-408.

## Journal Name

- 12 M.B. Kermani, M. Dougan, J.C. Gonzales, C. Linne, R. Cochrane. Eds., Development of low carbon Cr-Mo steels with exceptional corrosion resistance for oilfield applications, in: NACE International Corrosion Conference, Houston, USA, 2001.
- 13 L.N. Xu, S.Q. Guo, C.L. Gao, W. Chang, T.H. Chen and M.X. Lu, *Mater. Corros.*, 2013, 63, 997-1003.
- 14 J. Wang, C.N. Cao, J.J. Chen, M.D. Zhang, G.D. Ye and H.C. Lin, *Journal of Chinese Society for Corrosion and Protection*, 1995, 15, 241-246.
- 15 J. Wang, C.N. Cao, *Journal of Chinese Society for Corrosion and Protection*, 1996, 16, 9-14.
- 16 E. Desimoni, C. Malitesta and P.G. Zambonin, *Surf. Interface Anal.*, 1988, 13, 173-179.
- 17 T.P. Moffat, R.M. Latanision and R.R. Ruf, *Electrochimi. Acta*, 1995, 40, 1723-1734.